Spin-orbit-driven BCS-BEC crossover in a narrow Feshbach resonance

Kuang Zhang,[1] Gang Chen,[1,*] and Suotang Jia[1]

[1]*State Key Laboratory of Quantum Optics and Quantum Optics Devices, Laser spectroscopy Laboratory, Shanxi University, Taiyuan 030006, People's Republic of China*

In this paper we investigate the spin-orbit-driven BCS-BEC crossover physics in a narrow Feshbash resonance, and mainly focus on the bound state and the striking molecular signature based on a generalized two-channel model. For a weak spin-orbit coupling, only one bound state occurs. More importantly, we find two and more bound states in the case of the strong spin-orbit coupling. This bound-state number depends strongly on the strength, and especially, the type of spin-orbit coupling. The existence of the multi-bound states is a new phenomenon induced by spin-orbit coupling. In addition, we find that the molecular number does not vanish (but approaches zero) for a fixed positive detuning in the presence of spin-orbit coupling. When varying the strength of spin-orbit coupling in the positive detuning, an unconventional molecular signature that the molecular number increases and then decreases is revealed. We believe that in experiments our predicted molecular behavior is a good signature to detect the spin-orbit-induced superfluid physics.

PACS numbers: 03.75. Ss, 05.30. Fk, 67.85. Lm

Owing to their unprecedented level of control and precision, the investigation of spin-orbit (SO) coupling in the neutral atoms has attracted much attentions [1]. Especially, a one-dimensional (1D) equal Rashba and Dresselhaus SO coupling has been first realized in the ultracold ^{87}Rb atoms by a couple of Raman lasers [2]. Recently, the same SO coupling has been also created experimentally in degenerate Fermi gas with ^{40}K [3] and ^{6}Li [4]. In the presence of SO coupling, the degenerate Fermi gas has exhibited the interesting superfluid physics in both three [5–21] and lower dimensions [22–29]. For example, by increasing the strength of a Rashba SO coupling, the Cooper paring gap can be enhanced significantly attributed to the increased density of state at the Fermi surface. More importantly, this system may change from the Bardeen-Cooper-Schrieffer (BCS) superfluid to the Bose-Einstein condensate (BEC) with a new two-body bound state called Rashbon [5, 8], even on the BCS side with a negative scattering. When the effective Zeeman field is applied, the 2D degenerate Fermi gas with the Rashba SO coupling has an exotic topological superfluid supporting the Majorana fermions [23], which is the heart for realizing the topological quantum computing [30]. Recently, a universal midgap bound state in topological superfluids, which is induced by either nonmagnetic or magnetic impurities in the strong scattering limit, has been predicted [31].

For illustrating the SO-driven BCS-BEC crossover physics, a one-channel model, in which only the atoms tuned via Feshbash-resonant technique are taken into account, has been introduced in the previous considerations [5–29]. However, in degenerate Fermi gas, this one-channel model is valid for a *broad* Feshbash-resonant regime $\Gamma \gg 1$ [32], where $\Gamma = \sqrt{32m\mu_{\rm B}a_{\rm bg}^2B_{\rm w}^2/(\hbar^2\pi E_{\rm F})}$ is the dimensionless parameter, $\mu_{\rm B}$ is the Bohr magneton, m is the atom mass, $a_{\rm bg}$ is the background s-wave scattering strength, $B_{\rm w}$ is the resonant width and $E_{\rm F}$ is the Fermi energy. In fact, to get a more realistic and complete description of the BCS-BEC crossover physics, especially in a *narrow* Feshbash-resonant limit $\Gamma \ll 1$, a two-channel model, which includes both the atoms in the open channel and the molecules in the closed channel, must be introduced [33–36]. In the narrow Feshbash-resonant regime, some fundamental properties can be observed experimentally by detecting the striking molecular signature [37], additional to measuring the superfluid pairing gap applied usually in the one-channel model [38]. More importantly, new quantum phase transitions can be predicted [39, 40], due to the existence of extra U(1) symmetry for the molecular field.

On the experimental side, the degenerate Fermi gas in the narrow Feshbach resonant regime has been reported successfully in ^{6}Li [41] and the Fermi-Fermi mixture of ^{6}Li and ^{40}K [42]. Thus, it is crucially important to explore the SO-induced superfluid physics in this regime. In this paper we investigate the bound state and the molecular signature based on the SO-driven two-channel model in three dimensions. Our results are given as follows. (I) For a weak SO coupling, only one bound state can be found, which is identical to the result without SO coupling. (II) More importantly, we obtain two and more bound states, whose number depends strongly on the strength of SO coupling, in the case of the strong SO coupling. We also show that the bound-state number is affected deeply by the type of SO coupling, i.e., the number of the 1D equal Rashba-Dresselhaus SO coupling is more than that of the 2D Rashba case. (III) In addition, in the presence of SO coupling, the molecular number does not vanish (but approaches zero) even in the positive detuning. When varying the strength of SO coupling in the positive detuning, an unconventional molecular signature that the molecular number increases and then decreases is revealed. We believe that in experiments our predicted molecular behavior is a good signa-

*Corresponding author: chengang971@163.com

ture to detect the SO-induced superfluid physics.

Model and Hamiltonian–For the SO-driven two-channel model, the total Hamiltonian can be written formally as

$$H = H_{\rm F} + H_{\rm M} + H_{\rm I} + H_{\rm S}. \tag{1}$$

In Hamiltonian (1), $H_{\rm F} = \sum_{\mathbf{k}\sigma} \xi_{\mathbf{k}} C^{\dagger}_{\mathbf{k}\sigma} C_{\mathbf{k}\sigma}$ is the atom Hamiltonian, where $C^{\dagger}_{\mathbf{k}\sigma}$ is the creation operator for a atom with momentum $\mathbf{k}$, $\sigma = \uparrow, \downarrow$, $\xi_{\mathbf{k}} = \epsilon_{\mathbf{k}} - \mu$, $\epsilon_{\mathbf{k}} = k^2/(2m)$ is the kinetic energy, and μ is the chemical potential. $H_{\rm M} = \sum_{\mathbf{q}} (\epsilon_{\mathbf{q}} + \delta_0 - 2\mu) b^{\dagger}_{\mathbf{q}} b_{\mathbf{q}}$ is the molecular Hamiltonian, where $b^{\dagger}_{\mathbf{q}}$ is the creation operator of a molecule with momentum $\mathbf{q}$, $\epsilon_q = \hbar^2 q^2/(2M)$ with $M = 2m$ is the kinetic energy of molecule, and δ_0 is bare detuning determined by the position δ of the Feshbash resonance via a relation $\delta_0 = \delta + g^2 \sum_{\mathbf{k}} 1/(2\epsilon_{\mathbf{k}})$. At lower energy, the position is given approximately by $\delta \simeq 2\mu_{\rm B}(B - B_0)$, where B_0 is the magnetic field at which the resonance is at zero energy, and B is the tunable magnetic field [43]. The atom-molecule interconversion term is governed by the following Hamiltonian $H_{\rm I} = g \sum_{\mathbf{q}\mathbf{k}\mathbf{k}'} b^{\dagger}_{\mathbf{q}} C_{-\mathbf{k}+\frac{\mathbf{q}}{2}\downarrow} C_{\mathbf{k}+\frac{\mathbf{q}}{2}\uparrow} + C^{\dagger}_{\mathbf{k}'+\frac{\mathbf{q}}{2}\uparrow} C^{\dagger}_{-\mathbf{k}'+\frac{\mathbf{q}}{2}\downarrow} b_{\mathbf{q}}$, where g is the coupling constant that measures the amplitude of the decay of the molecule in the closed channel into a pair of the open-channel atoms. Finally, the SO coupling is chosen as a generalized Rashba and Dresselhaus type with Hamiltonian $H_{\rm S} = \alpha \sum_{\mathbf{k}} [(k_y + i\lambda k_x) C^{\dagger}_{\mathbf{k}\uparrow} C_{\mathbf{k}\downarrow} + (k_y - i\lambda k_x) C^{\dagger}_{\mathbf{k}\downarrow} C_{\mathbf{k}\uparrow}]$, where $\alpha = (\alpha_R + \alpha_D)$ is a generalized strength of SO coupling, α_R and α_D are the strengths of SO coupling for Rashba and Dresselhaus types, respectively, $\lambda = (\alpha_R - \alpha_D)/(\alpha_R + \alpha_D)$ determines the type of SO coupling. For example, for $\lambda = 1$ ($\alpha_D = 0$), the 2D Rashba SO coupling can be found. Whereas, for $\lambda = 0$ ($\alpha_D = \alpha_R$), the 1D equal Rashba and Dresselhaus SO coupling can be generated. Fortunately, this equal SO coupling has been realized experimentally in the ultracold neutral atoms [2–4].

In the absence of SO coupling ($\alpha = 0$), Hamiltonian (1) reduces to the standard two-channel model [33–36], in which only the singlet Cooper paring can be formed. However, in the presence of SO coupling, the result is quite different. A crucial difference is that the singlet and triplet Cooper parings can coexist. As a result, the system exhibits rich bound states and unconventional molecular signature, as will be shown. For simplicity, we mainly focus on the case of $\mathbf{q} = \mathbf{0}$ in the following discussions.

Two-body bound state–We begin to discuss the two-body bound state for the two-channel model driven by the generalized SO coupling from an ansatz wavefunction of the total Hamiltonian (1). Due to existence of the singlet and triplet Cooper parings, the ansatz wavefunction should be written formally as

$$|\Psi\rangle = \Big(\sum_{k'\sigma\sigma'} \beta_{k'\sigma\sigma'} C^{\dagger}_{\mathbf{k}'\sigma} C^{\dagger}_{\mathbf{k}'\sigma'} + \gamma b^{\dagger}_0 \Big) |0,0,0,0\rangle \otimes |0\rangle , \tag{2}$$

where $\beta_{k'\uparrow\downarrow}$ and $\beta_{k'\downarrow\uparrow}$ ($\beta_{k'\uparrow\uparrow}$ and $\beta_{k'\downarrow\downarrow}$) represent the amplitude of probability for the singlet (triplet) Cooper paring, γ represents the amplitude of probability of the molecule, and $|0,0,0,0\rangle \otimes |0\rangle$ is the direct multiple of the fermion vacuum with spin flipping and molecule vacuum. Substituting the wavefunction in Eq. (2) into the stationary Schrödinger equation $(H - E)|\Psi\rangle = 0$, we find that the six coefficients including the energy E satisfy the following equations:

$$\begin{cases} g\gamma + \beta_{k'\uparrow\uparrow}\alpha k_- = \Xi_k \beta_{k\downarrow\uparrow} \\ g\gamma + \beta_{k'\downarrow\downarrow}\alpha k_+ = \Xi_k \beta_{k\uparrow\downarrow} \\ (\beta_{k'\downarrow\uparrow} + \beta_{k'\uparrow\downarrow})\alpha k_+ = \Xi_k \beta_{k'\uparrow\uparrow} \\ (\beta_{k'\downarrow\uparrow} + \beta_{k'\uparrow\downarrow})\alpha k_- = \Xi_k \beta_{k'\downarrow\downarrow} \\ 2(\delta_0 - E)\gamma = -g \sum_{k'} (\beta_{k'\uparrow\downarrow} + \beta_{k'\downarrow\uparrow}) \end{cases}, \tag{3}$$

where $\Xi_k = E - 2\epsilon_k$ and $k_{\pm} = k_y \pm i\lambda k_x$. Eq. (3) can not be solved directly because of lack of a coefficient equation. If we define the spin symmetry and anti-symmetry vectors as $\psi_s(k) = (\beta_{k\downarrow\uparrow} - \beta_{k\uparrow\downarrow})/\sqrt{2}$ and $\psi_a(k) = (\beta_{k\downarrow\uparrow} + \beta_{k\uparrow\downarrow})/\sqrt{2}$, the stationary Schrödinger equation is rewritten in the representation of $\psi_k = [\beta_{k\uparrow\downarrow}, \beta_{k\downarrow\uparrow}, \beta_{k\downarrow\downarrow}, \beta_{k\uparrow\uparrow}, \gamma]^T$ as $(H - E)\psi_k = 0$, which leads to another equations for the coefficients $\beta_{k'\sigma,\sigma'}$ and γ, that is, $\gamma = -g\sqrt{2}\sum_{k'} \psi_a(k')/(\delta_0 - E)$, $\beta_{k'\uparrow\uparrow} = \sqrt{2}\psi_a(k)\alpha k_+/\Xi_k$, and $\beta_{k'\downarrow\downarrow} = \sqrt{2}\psi_a(k)\alpha k_-/\Xi_k$. Substituting these obtained equations into Eq. (3) yields

$$\sum_k \Big(\frac{\Xi_k}{\Xi_k^2 - 4\alpha^2 k_+ k_-} + \frac{1}{2\epsilon_k} \Big) = \frac{E - \delta}{g^2}. \tag{4}$$

Equation (4) is responsible for the bound state for our considered two-channel model with the generalized SO coupling. From Eq. (4) we can derive the energy E. However, in order to prove the real bound state, we must cooperate with the condition $E < E_T$, where $E_T = \frac{m\alpha^2}{\hbar^2}[\frac{1+\lambda^2}{2} - (1 + \lambda)]$ is called the threshold energy for the total Hamiltonian (1) [5]. In the absence of SO coupling ($\alpha = 0$), this threshold energy becomes $E_T = 0$, as expected. In the following discussions, we mainly consider two interesting cases, including the 2D Rashba ($\lambda = 1$) and 1D equal Rashba and Dresselhaus ($\lambda = 0$) SO couplings realized by the recent experiments [2–4], to reveal the fundamental properties for the bound state.

We first address the case of the 2D Rashba SO coupling. In the absence of SO coupling, i.e., $\alpha = 0$, the analytical bound-state energy is derived from Eq. (4) by $E = (-g^4 m^3 + 32\pi^2\delta - g^2\sqrt{g^2 m^6 - 64 m^3 \pi^2 \delta})/(32\pi^2)$. It implies that in such a case only one bound state can be found [32]. In the presence of SO coupling, the explicit expression for the bound-state energy can not be obtained. However, for a weak SO coupling, Eq. (4) is simplified as $2m^{\frac{3}{2}}(E + m\alpha^2)/(8\pi\sqrt{-E}) = (E - \delta)/g^2$ with the help of a Taylor expansion with respect to the strength of SO coupling. In this case, Hamiltonian (1) also exhibits one bound state, as shown in Fig. 1(a).

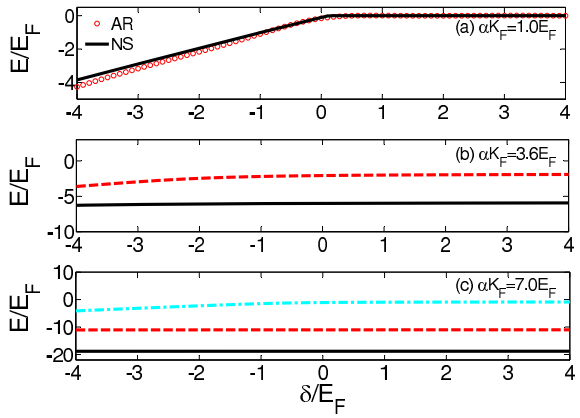

FIG. 1: (Color online) The bound-state energy for the 2D Rashba SO coupling ($\lambda = 1$) as a function of the detuning δ for the different strengths of SO coupling (a) $\alpha K_{\rm F} = 1.0E_{\rm F}$, (b) $\alpha K_{\rm F} = 3.6E_{\rm F}$ and (c) $\alpha K_{\rm F} = 7.0E_{\rm F}$ when $\Gamma = 0.1$. In Fig. 1(a), the red open symbol corresponds to the analytical result (AR) and the black solid line represents the direct numerical simulation (NS).

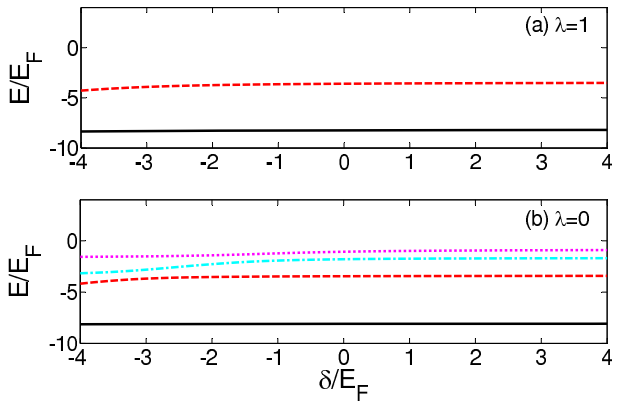

FIG. 2: (Color online) The bound-state energy as a function of the detuning δ for the different types of SO coupling including (a) $\lambda = 1$ (2D Rashba) and (b) $\lambda = 0$ (1D equal Rashba and Dresselhaus), when $\Gamma = 0.1$ and $\alpha K_{\rm F} = 4.2E_{\rm F}$.

By further solving the above equation approximately, we find that the bound-state energy is proportional to $-\alpha^4$. This behavior agrees well with the numerical simulation, as also shown in Fig. 1(a), and implies that the bound-state energy can decrease by increasing the strength of SO coupling. For the strong SO coupling, the perturbation method is invalid. Here we numerically solve Eq. (4) to evaluate the energy E. Quite surprisingly, Hamiltonian (1) has two bound states in the strong SO coupling, as shown in Fig. 1(b). Moreover, the bound-state number depends strongly on the strength of SO coupling , i.e., when increasing the strength of SO coupling, the bound-state number increases, as shown in Fig. 1(c). The existence of the multi-bound states is a new phenomenon induced by SO coupling and may generate exotic superfluid physics.

Another important observation of Eq. (4) is that the bound-state number is affected deeply by the type of SO coupling. In Fig. 2, we plot the bound-state energy with respect to the detuning δ for the different types of SO coupling including (a) $\lambda = 1$ (2D Rashba) and (b) $\lambda = 0$ (1D equal Rashba and Dresselhaus). It can be seen clearly that for a fixed strong SO coupling, the bound-state number for the 1D equal Rashba and Dresselhaus SO coupling is more than that of the 2D Rashba SO coupling. In order to prove this argument again, we numerically calculate the bound-state number in the range of the strength αK_F of SO coupling from 0 to $6.4E_F$ when $\Gamma = 0.1$ and $\delta = -3E_F$. We find approximately that for the 2D Rashba SO coupling, the bound-state number is given by $N_{\rm R} = 1$ for $\alpha K_F/E_F \in [0.0, 3.0]$ and $N_{\rm R} = 2$ for $\alpha K_F/E_F \in [3.1, 6.4]$. Whereas, for the 1D equal Rashba and Dresselhaus SO coupling, the bound-state number becomes $N_{\rm RD} = 1$ for $\alpha K_F/E_F \in [0.0, 2.9]$, $N_{\rm RD} = 2$ for $\alpha K_F/E_F \in [3.0, 3.5]$, $N_{\rm RD} = 3$ for $\alpha K_F/E_F \in [3.6, 3.9]$, $N_{\rm RD} = 4$ for $\alpha K_F/E_F \in [4.0, 4.9]$, $N_{\rm RD} = 5$ for $\alpha K_F/E_F \in [5.0, 5.4]$, and $N_{\rm RD} = 6$ for $\alpha K_F/E_F \in [5.5, 6.4]$.

Molecular signature–After discussing the bound state driven by SO coupling in the two-channel model, now we explore the experimentally-measurable molecular signature. In terms of the Hellmann-Feymann theorem, the molecular number is obtained by

$$N_0 = \langle\Psi| b_{\mathbf{0}}^\dagger b_{\mathbf{0}} |\Psi\rangle = \langle\Psi| \frac{\partial H}{\partial \delta_0} |\Psi\rangle = \frac{dE}{d\delta}, \qquad (5)$$

where the bound-state energy E can be derived from Eq. (4), together with the condition $E < E_T$. Here we are interested in the regime for the one bound state.

In Fig. 3 we plot the scaled molecular number $2N_0/N$ of both the 2D Rashba and the 1D equal Rashba and Dresselhaus SO couplings with respect to the detuning δ for the different strengths of SO coupling. In the absence of SO coupling ($\alpha K_{\rm F} = 0$), the striking molecular signature can be found in the case of the negative detuning ($\delta < 0$). However, for the positive detuning ($\delta > 0$), the physical bound state disappears [44], and thus there is no real molecular number, as shown in black solid line of Fig. 3. With the increasing of the strength of SO coupling, the molecular number in the negative detuning decreases, as shown in red dash line of Fig. 3. The physics can be understood as follows. In the two channel model, the molecules play two roles. One is that they interact directly with the atoms via Hamiltonian $H_{\rm I}$. The other (the most important) is that they induce the indirect atom-atom interactions, which generate the Cooper pairing. When the SO coupling enhances the Cooper pairing [6–8], the molecules are thus suppressed because the system need guarantee a conserved number $N = 2b_{\mathbf{0}}^\dagger b_{\mathbf{0}} + \sum_{\mathbf{k}\sigma} C_{\mathbf{k}\sigma}^\dagger C_{\mathbf{k}\sigma}$. On the other hand, in the presence of SO coupling, there still exists a large molecular signature in the positive detuning, which is contrast

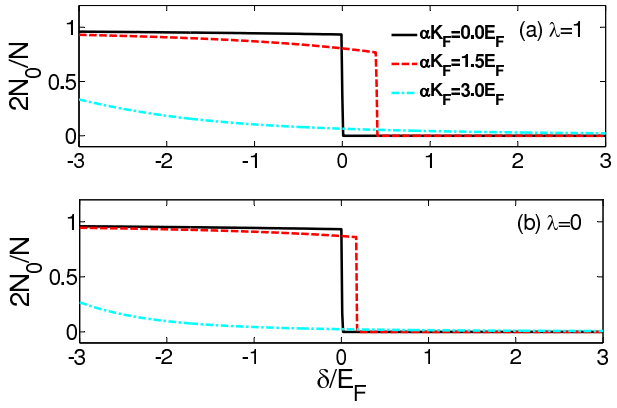

FIG. 3: (Color online) The molecular number of both (a) the 2D Rashba SO coupling with $\lambda = 1$ and (b) the 1D equal Rashba and Dresselhaus SO coupling with $\lambda = 0$ as a function of the detuning δ for the different strengths of SO coupling $\alpha K_{\rm F} = 0.0E_{\rm F}$ (Black solid line), $\alpha K_{\rm F} = 1.5E_{\rm F}$ (Red dashed line) and $\alpha K_{\rm F} = 3.0E_{\rm F}$ (Cyan dash-dotted line) when $\Gamma = 0.1$.

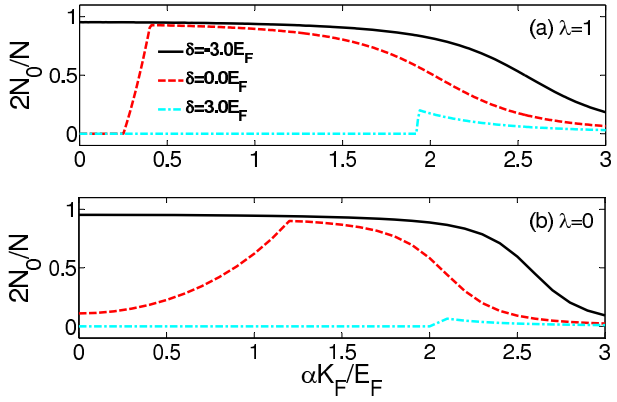

FIG. 4: (Color online) The molecular number of both (a) the 2D Rashba SO coupling with $\lambda = 1$ and (b) the 1D equal Rashba and Dresselhaus SO coupling with $\lambda = 0$ as a function of the strength $\alpha K_{\rm F}$ of SO coupling for the different detungings $\delta = -3.0E_{\rm F}$ (Black solid line), $\delta = 1.5E_{\rm F}$ (Red dashed line) and $\delta = 3.0E_{\rm F}$ (Cyan dash-dotted line) when $\Gamma = 0.1$.

to the result without SO coupling. Finally, by means of the perturbation method, the molecular number is obtained as $2N_0/N = C_1 + C_2\alpha^2$, where C_1 and C_2 are the complicate coefficients independent of the strength of SO coupling. In the absence of SO coupling, $C_1 \equiv 0$ for $\delta \geq 0$ and $C_1 \simeq 1$ for $\delta < 0$. This analytical expression shows that the molecular number does not vanish (but approaches zero) for a positive detuning in the presence of SO coupling, as shown in cyan dash-dotted line of Fig. 3.

In Fig. 4, we plot the molecular number of both the 2D Rashba and the 1D equal Rashba and Dresselhaus SO couplings with respect to the strength of SO coupling for the different detunings. In the negative detuning ($\delta < 0$) we shows again that the SO coupling suppresses the molecular number (black solid line of Fig. 4). However, for the zero and positive detunings ($\delta \geq 0$), we find that the molecular number increases and then decreases, and eventually, approaches zero, when increasing the strength of SO coupling. Moreover, with the increasing of the negative detuning, the corresponding peak of the molecular number decreases. In contrast to the pairing gap that varies smoothly as a function of the strength of SO coupling [6–8], we believe that in experiments our predicted unconventional behavior for the molecular number is a good signature to detect the SO-induced superfluid physics.

Conclusions–In summary, motivated by the recent experimental developments about the degenerate Fermi gas, we have investigated the SO-driven BCS-BEC crossover in the narrow Feshbash resonance based on the generalized two-channel model. We have found that the SO coupling can generate rich bound states and unconventional molecular signature. In experiments, we believe that our predicted molecular behavior is a good signature to detect the SO-induced superfluid physics. In addition, since the multi-bound states can promote fluctuations and possibly inhibit condensation, some SO-induced exotic phenomena may occur in the narrow Feshbash resonance.

We thank Professors Peng Zhang, Wei Yi, Shizhong Zhang and Doctor Zengqiang Yu for their helpful discussions. This work was supported partly by the 973 program under Grant No. 2012CB921603; the NNSFC under Grants No. 10934004, No. 11074154, and No. 61275211; NNSFC Project for Excellent Research Team under Grant No. 61121064; and International Science and Technology Cooperation Program of China under Grant No.2001DFA12490.

Note added–During preparing this paper, we noticed that two bound states for the SO-driven two-channel model was also predicted by V. B. Shenoy in terms of a renormalizable quantum field theory [45]. Our results can agree with each other where they overlap.

[1] J. Dalibard, F. Gerbier, G. Juzeliūnas, and P. Öhberg, Rev. Mod. Phys. **83**, 1523 (2011).
[2] Y. -J. Lin, K. Jimenez-Garcia, and I. B. Spielman, Nature (London), **471**, 83 (2011).
[3] P. Wang, Z. -Q. Yu, Z. Fu, J. Miao, L. Huang, S. Chai, H. Zhai, and J. Zhang, Phys. Rev. Lett. **109**, 095301 (2012).
[4] L. W. Cheuk, A. T. Sommer, Z. Hadzibabic, T. Yefsah, W. S. Bakr, and M. W. Zwierlein, Phys. Rev. Lett. **109**, 095302 (2012).
[5] J. P. Vyasanakere and V. B. Shenoy, Phys. Rev. B **83**,

094515 (2011).
[6] M. Gong, S. Tewari, and C. Zhang, Phys. Rev. Lett. **107**, 195303 (2011).
[7] Z. -Q. Yu, and H. Zhai, Phys. Rev. Lett. **107**, 195305 (2011).
[8] H. Hu, L. Jiang, X. -J. Liu, and H. Pu, Phys. Rev. Lett. **107**, 195304 (2011).
[9] J. P. Vyasanakere, S. Zhang, and V. B. Shenoy, Phys. Rev. B **84**, 014512 (2011).
[10] M. Iskin, and A. L. Subasi, Phys. Rev. Lett. **107**, 050402 (2011); Phys. Rev. A **84**, 043621 (2011).
[11] L. Jiang, X. -J. Liu, H. Hu, and H. Pu, Phys. Rev. A **84**, 063618 (2011).
[12] W. Yi, and G. -C. Guo, Phys. Rev. A **84**, 031608 (2011).
[13] L. Dell'Anna, G. Mazzarella, and L. Salasnich, Phys. Rev. A **84**, 033633 (2011); Phys. Rev. A **86**, 053632 (2012).
[14] L. Han, and C. A. R. Sá de Melo, Phys. Rev. A **85**, 011606 (2012).
[15] K. Seo, L. Han, and C. A. R. Sá de Melo, Phys. Rev. Lett. **109**, 105303 (2012); Phys. Rev. A **85**, 033601 (2012); arXiv:1301.1353 (2013).
[16] K. Zhou and Z. Zhang, Phys. Rev. Lett. **108**, 025301 (2012).
[17] R. Liao, Y. -X. Yu, and W. -M. Liu, Phys. Rev. Lett. **108**, 080406 (2012).
[18] P. Zhang, L. Zhang, and Y. Deng, Phys. Rev. A **86**, 053608 (2012).
[19] P. Zhang, L. Zhang, and W. Zhang, Phys. Rev. A **86**, 042707 (2012).
[20] L. He and X. -G. Huang, Phys. Rev. B **86**, 014511 (2012).
[21] L. Dong, L. Jiang, H. Hu, and H. Pu, arXiv:1211.1700 (2012).
[22] G. Chen, M. Gong, and C. Zhang, Phys. Rev. A **85**, 013601 (2012).
[23] M. Gong, G. Chen, S. Jia, and C. Zhang, Phys. Rev. Lett. **109**, 105302 (2012).
[24] L. He and X. -G. Huang, Phys. Rev. Lett. **108**, 145302 (2012); Phys. Rev. A **86**, 043618 (2012).
[25] J. Zhou, W. Zhang, and W. Yi, Phys. Rev. A **84**, 063603 (2012).
[26] W. Yi and W. Zhang, Phys. Rev. Lett. **109**, 140402 (2012).
[27] X. Yang and S. Wan, Phys. Rev. A **85**, 023633 (2012).
[28] J. -N. Zhang, Y. -H. Chan, and L. -M. Duan, arXiv:1110.2241 (2011).
[29] F. Wu, G. -C. Guo, W. Zhang, and W. Yi, arXiv:1211.5780 (2012).
[30] C. Nayak, S. H. Simon, A. Stern, M. Freedman, and S. Das Sarma, Rev. Mod. Phys. **80**, 1083 (2008).
[31] H. Hu, L. Jiang, H. Pu, Y. Chen, and X. -J. Liu, Phys. Rev. Lett. **110**, 020401 (2013).
[32] D. E. Sheehy and L. Radzihovsky, Phys. Rev. Lett. **96**, 060401 (2006); Ann. Phys. **322**, 1790 (2007).
[33] M. Holland, S. J. J. M. F. Kokkelmans, M. L. Chiofalo, and R. Walser, Phys. Rev. Lett. **87**, 120406 (2001).
[34] E. Timmermans, K. Furuya, P. W. Milonni, and A. K. Kerman, Phys. Lett. **A 285**, 228 (2001).
[35] Y. Ohashi and A. Griffin, Phys. Rev. Lett. **89**, 130402 (2002).
[36] R. Duine and H. Stoof, Phys. Rep. **396**, 115 (2004).
[37] G. B. Partridge, K. E. Strecker, R. I. Kamar, M. W. Jack, and R. G. Hulet, Phys. Rev. Lett. **95**, 020404 (2005).
[38] S. Giorgini, L. P. Pitaevskii, and S. Stringari, Rev. Mod. Phys. **80**, 1215 (2008)
[39] Y. Nishida, Phys. Rev. Lett. **109**, 240401 (2012).
[40] Z. Shen, L. Radzihovsky, and V. Gurarie, Phys. Rev. Lett. **109**, 245302 (2012).
[41] E. L. Hazlett, Y. Zhang, R.W. Stites, and K. M. O'Hara, Phys. Rev. Lett. **108**, 045304 (2012).
[42] L. Costa, J. Brachmann, A. -C. Voigt, C. Hahn, M. Taglieber, T. W. Hänsch, and K. Dieckmann, Phys. Rev. Lett. **105**, 123201 (2010).
[43] C. Chin, R. Grimm, P. Julienne, and E. Tiesinga, Rev. Mod. Phys. **82**, 1225 (2010).
[44] L. D. Landau and E. M. Lifshitz, *Quantum Mechanics: Non-relativistic Theory* (Permagon, New York, 1977).
[45] V. B. Shenoy, arXiv: 1212. 2858 (2012).